First experimental photoelectron spectra of superhalogens and their theoretical interpretations

Xue-Bin Wang, Chuan-Fan Ding, and Lai-Sheng Wang[a)]
Department of Physics, Washington State University, Richland, Washington 99352, and W. R. Wiley Environmental Molecular Sciences Laboratory, Pacific Northwest National Laboratory, MS K8-88, P.O. Box 999, Richland, Washington 99352

Alexander I. Boldyrev and Jack Simons
Department of Chemistry, The University of Utah, Salt Lake City, Utah 84112

(Received 28 October 1998; accepted 4 December 1998)

Photoelectron spectra of the MX_2^- (M=Li, Na; X=Cl, Br, I) superhalogen anions have been obtained for the first time. The first vertical detachment energies (VDEs) were measured to be 5.92±0.04 ($LiCl_2^-$), 5.86±0.06 ($NaCl_2^-$), 5.42±0.03 ($LiBr_2^-$), 5.36±0.06 ($NaBr_2^-$), 4.88±0.03 (LiI_2^-), and 4.84±0.06 eV (NaI_2^-), which are all well above the 3.61 eV electron detachment energy of Cl^-, the highest among atomic anions. Experimental photoelectron spectra have been assigned on the basis of *ab initio* outer valence Green function (OVGF) calculations. The corresponding theoretical first VDEs were found to be 5.90 ($LiCl_2^-$), 5.81 ($NaCl_2^-$), 5.48 ($LiBr_2^-$), 5.43 ($NaBr_2^-$), 4.57 (LiI_2^-), and 4.50 eV (NaI_2^-), in excellent agreement with the experimental values. Photodetachment from the top four valence molecular orbitals ($2\sigma_g^2 2\sigma_u^2 1\pi_u^4 1\pi_g^4$) of MX_2^- was observed. Analysis of the polestrength showed that all electron detachment channels in this study can be described as primarily one-electron processes. © *1999 American Institute of Physics.* [S0021-9606(99)01010-7]

I. INTRODUCTION

Molecules with high electron affinities (EAs) play a very important role in chemistry. For example, in 1962, Bartlett synthesized the first chemically bound xenon in $Xe^+[PtF_6]^-$.[1] This milestone work started the Chemistry of Nobel Gases, which previously have been considered as absolutely inert atoms. Since then, numerous molecules with high EAs were used to synthesize a wide variety of new chemical compounds, in which very strong oxidizers were required. Even today, molecules with high EAs continue to be employed in the preparation of many new materials, including organic metals and organic superconductors.[2]

Halogen atoms possess the highest EAs (3.0–3.6 eV) among all the atoms.[3] However, molecules may exceed the 3.6 eV limit due to collective effects. There is a class of molecules, known as superhalogens[4,5] that are especially important oxidizers. The EAs of many superhalogens have been estimated both theoretically[4–34] and experimentally.[35–59] In 1981 Gutsev and Boldyrev proposed a simple formula for one class of superhalogens, MX_{k+1}, where M is a main group or transition metal atom, X is a halogen atom, and k is the maximal formal valence of the atom M.[4] Some superhalogen anions, such as BF_4^-, $AlCl_4^-$, ScF_4^-, $SiCl_5^-$, TaF_6^-, and AsF_6^-, are commonly found as building blocks in condensed phase materials and gas phase molecules. These anions have extremely high electron detachment energies due to the delocalization of the extra electron over the electronegative halogen atoms in the closed shell anions. While these anions are well characterized in condensed phases, their gas-phase electron detachment energies have *not yet been measured* experimentally. There are two main reasons for this: (1) the low stability of the neutral counterparts, making the Knudsen-type equilibrium experiments very difficult for these anions; (2) their very high electron detachment energies, making it very difficult to perform direct photodetachment experiments using photoelectron spectroscopy (PES).

Recently, we have developed a new experimental facility, which couples a magnetic-bottle time-of-flight (TOF) photoelectron spectroscopy apparatus and an electrospray ionization (ESI) source.[60] The aim of this apparatus is to investigate multiply charged anions.[61–63] However, we have found that it is also ideal for investigating superhalogens because the ESI source is perfectly suitable for producing the superhalogen anions. The high sensitivity of the magnetic-bottle PES technique allows high photon energy experiments to be conveniently performed. In this work, we report the first experimental photoelectron spectra of the smallest superhalogens for the MX_{k+1}^- class of molecules, where M=Li and Na and X=Cl, Br, and I.

Although early DVM-X_α calculations[4,5] substantially underestimated the vertical detachment energies (VDEs) of these superhalogen anions, they were able to find that the VDEs of these species were higher than 3.6 eV and confirmed their superhalogen nature. More recent and accurate calculations, using Green's function and coupled-cluster single double triple [CCSD(T)] methods, yielded substantially higher values for the VDEs: LiF_2^- (6.80 eV;[16,21,23] 6.51 eV[33]), $LiCl_2^-$ (5.73 eV;[23] 5.88 eV[33]), NaF_2^- (6.54 eV;[23] 6.18 eV[33]), $NaCl_2^-$ (5.64 eV;[23] 5.77 eV[33]), KF_2^- (6.07 eV[23]), KCl_2^- (5.37 eV[23]). Adiabatic detachment energies (ADE) of LiF_2^- (5.45 eV[33]), $LiCl_2^-$ (4.97 eV[33]), NaF_2^- (5.12 eV[33]),

a)Electronic mail: LS.WANG@PNL.GOV

 © 1999 American Institute of Physics

Downloaded 23 May 2003 to 155.101.19.15. Redistribution subject to AIP license or copyright, see http://ojps.aip.org/jcpo/jcpcr.jsp

$NaCl_2^-$ (4.69 eV[33]) were also calculated at the CCSD(T) level of theory. However, results that have appeared in the literature are not sufficient to interpret our experimental photoelectron spectra. Therefore we performed additional calculations for $LiCl_2^-$ and $NaCl_2^-$ in this work. We further performed new calculations for the heavier superhalogens, LiX_2^- and NaX_2^- (X=Br and I), which were not studied previously.

The current work provides the first experimental verification of the high EAs for the MX_{k+1} superhalogens. The combination of the experimental and theoretical investigation provides a clear picture of the electronic structure of the superhalogens. This paper is organized as follows. In the next section, the experimental aspects are presented and in Sec. III the computational details are described. We report the experimental results in Sec. IV, followed by a detailed spectral assignment and discussion in Sec. V. Finally, a summary is given in Sec. VI.

II. EXPERIMENT

The experiments were carried out with our new photoelectron spectroscopy facility, which involves a magnetic-bottle TOF photoelectron analyzer and an ESI source.[60] Brief descriptions of this apparatus have been reported in our recent publications[61–63] and details will be published elsewhere.[60] To produce the desired anions, we used a 10^{-4} molar solution of the corresponding salts (LiCl, NaCl, LiBr, NaBr, LiI, and NaI) at pH=7 in a water/methanol mixed solvent (2/98 ratio). The solution was sprayed through a 0.01 mm diam syringe needle at ambient atmosphere and at a high voltage bias of −2.2 kV, producing highly charged liquid droplets which were fed into a desolvation capillary. Negatively charged molecular ions emerging from the desolvation capillary were guided by a radio frequency-only quadruple ion guide into an ion trap, where the ions were accumulated for 0.1 s before being pushed into the extraction zone of a TOF mass spectrometer. The major anions from the ESI source were of the form, $M_kX_{k+1}^-$, and their relative intensities depended on the source conditions. In the current experiments, we focus on the smallest species, MX_2^-.

In each PES experiment, the anions of interest were mass selected and decelerated before being intercepted by a laser beam in the detachment zone of the magnetic-bottle photoelectron analyzer. For the current study, photodetachment at 193 nm (6.424 eV) from an ArF excimer laser was used due to the high electron binding energies of the superhalogens. Photoelectron TOF spectra were collected for each anion and then converted to kinetic energy spectra, calibrated by the known spectra of I^- and O^-. The binding energy spectra were obtained by subtracting the kinetic energy spectra from the photon energy. The energy resolution was about 20 meV full width at half maximum (FWHM) at 0.4 eV kinetic energy, as measured from the spectrum of I^- at 355 nm and would deteriorate at higher kinetic energies.

III. COMPUTATIONAL DETAILS

In recent studies, Gutsev and others showed that reliable results for neutral superhalogens can be obtained only with the infinite-order coupled-cluster method at the all singles and doubles (CCSD) level with the noniterative inclusion of triple excitations CCSD(T).[64,65] Therefore in this study we employed the CCSD(T) method in all our geometry and frequency calculations using the GAUSSIAN-94 program.[66] Moderate-sized $6-311+G(d)$ basis sets[67–70] were used in these calculations for LiCl, $LiCl_2^-$, $LiCl_2$, NaCl, $NaCl_2^-$, $NaCl_2$, LiBr, $LiBr_2^-$, $LiBr_2$, NaBr, $NaBr_2^-$, and $NaBr_2$, and the core electrons were kept frozen in treating the electron correlation.

CCSD(T) geometry calculations for LiI, LiI_2^-, LiI_2, NaI, NaI_2^-, and NaI_2 were performed with basis sets constructed from the LANLDZ basis sets (incorporated in GAUSSIAN-94)[71,72] extended by a set of *sp* functions to make it triple-zeta quality [$\alpha(s,p)=0.56$ for Li, $\alpha(s,p)=0.19$ for Na, and $\alpha(s,p)=0.56$ for I], by a set of *d* functions [$\alpha(d)=0.19$ for Li, $\alpha(d)=0.13$ for Na, and $\alpha(d)=0.27$ for I] and by a set of diffuse *sp* functions on I [$\alpha(s,p)=0.03$]. The Los Alamos effective relativistic pseudopotentials were used to treat core electrons in these calculations (except Li, where all electrons were included in self-consistent field (SCF) calculations).[71,72] The additional *s*, *p*, *d* functions on Li and I were optimized using the MP2 total energy of the LiI molecule at the equilibrium bond length ($R_e=2.392$ Å). The *s*, *p*, and *d* functions on Na were optimized using the MP2 total energy of the NaI molecule at the equilibrium bond length ($R_e=2.711$ Å). The *s*, *p* diffuse functions on I were optimized using the MP2 total energy of I^-. The resulting basis sets (TZ+*d*+diff) were used in all calculations on the iodine-containing molecules. Frequency calculations were not performed at the CCSD(T)/TZ+*d*+diff level of theory because of a problem in the GAUSSIAN-94 program, which is unable to run CCSD(T) frequency calculations with pseudopotentials. The results of our calculations for LiCl, NaCl, LiBr, NaBr, LiI, and NaI together with experimental data are presented in Table I.

TABLE I. Calculated and experimental molecular properties of LiCl, NaCl, LiBr, NaBr, LiI, and NaI.

Molecule ($C_{\infty v}$, $^1\Sigma^+$)	Method	$E_{CCSD(T)}$ (a.u.)	R (M-X) (Å)	ω_e (cm^{-1})
LiCl	CCSD(T)/6–311+G*	−467.204 312	2.022	659
	Experiment[a]		2.020 673	643.31
NaCl	CCSD(T)/6–311+G*	−621.592 593	2.382	367
	Experiment[a]		2.360 795	366
LiBr	CCSD(T)/6–311+G*	−2580.052 965	2.188	569
	Experiment[a]		2.170 427	563.16
NaBr	CCSD(T)/6–311+G*	−2734.445 632	2.539	297
	Experiment[a]		2.502 038	302.1
LiI	CCSD(T)/TZ+*d*+diff	−18.829 475	2.419	
	Experiment[a]		2.391 924	498.16
NaI	CCSD(T)/TZ+*d*+diff	−11.558 204	2.766	
	Experiment[a]		2.711 452	258

[a]Reference 82.

VDEs of the superhalogen anions were calculated using the outer valence Green function (OVGF) method[73–77] incorporated in GAUSSIAN-94. The $6-311+G(2df)$ basis sets were used in the OVGF calculations of LiCl, $LiCl_2^-$, NaCl, $NaCl_2^-$, LiBr, $LiBr_2^-$, NaBr, $NaBr_2^-$, and the TZ+*d*+diff

Downloaded 23 May 2003 to 155.101.19.15. Redistribution subject to AIP license or copyright, see http://ojps.aip.org/jcpo/jcpcr.jsp

TABLE II. Experimental and calculated vertical ionization potentials (IP, eV) of LiCl and NaCl.

Ionization transitions: $MX\ (^1\Sigma^+) \rightarrow MX^+$ or $MX^-\ (^2\Sigma^+) \rightarrow MX$	IP (exp.)	IP (theo.)[d] OVGF/6–311+ G(2df)+Corr.	IP (theo.)[e] OVGF/6–311+ G(2df)
LiCl			
$X\ ^2\Pi_{3/2}(2\sigma^2 1\pi^3)$	9.965[a]	10.03	10.06 (0.923) ($^2\Pi$)
$^2\Pi_{1/2}$	10.024[a]	10.09	
$^2\Sigma^+(2\sigma^1 1\pi^4)$	10.71[a]	10.69	10.69 (0.917) ($^2\Sigma^+$)
$LiCl^-$			
$X\ ^2\Sigma^+(2\sigma^2 1\pi^4 3\sigma^1)$	0.593[b]	0.52	0.52 (0.994) ($^2\Sigma^+$)
NaCl			
$X\ ^2\Pi_{3/2}(2\sigma^2 1\pi^3)$	9.34[c]	9.17	9.20 (0.917) ($^2\Pi$)
$^2\Pi_{1/2}$		9.23	
$^2\Sigma^+(2\sigma^1 1\pi^4)$	9.80[c]	9.63	9.63 (0.917) ($^2\Sigma^+$)
$NaCl^-$			
$X\ ^2\Sigma^+(2\sigma^2 1\pi^4 3\sigma^1)$	0.727[b]	0.62	0.62 (0.995) ($^2\Sigma^+$)

[a]Reference 83.
[b]Reference 84.
[c]Reference 85.
[d]Spin-orbit correction was added on the basis of the experimental $^2\Pi_{3/2}$ and $^2\Pi_{1/2}$ splitting in LiCl (Ref. 83).
[e]Polestrength is given in parentheses.

basis sets were used in the OVGF calculations of LiI, LiI_2^-, NaI and NaI_2^-. For the superhalogens studied here, one may expect an appreciable spin-orbit splitting, especially for compounds containing Br and I. To incorporate such spin-orbit splitting in our interpretational scheme, we first performed OVGF calculations of diatomic molecules: LiCl, NaCl, LiBr, NaBr, LiI, and NaI without spin-orbit coupling. From experimental data of these molecules we then estimated spin-orbit couplings. The spin-orbit uncorrected and corrected OVGF results based on the experimental spin-orbit couplings together with experimental data are presented in Tables II–IV for the diatomic molecules.

TABLE III. Experimental and calculated vertical ionization potentials (IP, eV) of LiBr and NaBr.

Ionization transitions: $MX\ (^1\Sigma^+) \rightarrow MX^+$ or $MX^-\ (^2\Sigma^+) \rightarrow MX$	IP (exp.)	IP (theo.)[d] OVGF/6–311+ G(2df)+Corr.	IP (theo.)[e] OVGF/6–311+ G(2df)
LiBr			
$X\ ^2\Pi_{3/2}(2\sigma^2 1\pi^3)$	9.279[a]	9.29	9.36 (0.920) ($^2\Pi$)
$^2\Pi_{1/2}$	9.416[a]	9.43	
$^2\Sigma^+(2\sigma^1 1\pi^4)$	10.28[a]	10.04	10.11 (0.919) ($^2\Sigma^+$)
$LiBr^-$			
$X\ ^2\Sigma^+(2\sigma^2 1\pi^4 3\sigma^1)$		0.58	0.58 (0.992) ($^2\Sigma^+$)
NaBr			
$X\ ^2\Pi_{3/2}(2\sigma^2 1\pi^3)$	8.80[c]	8.64	8.71 (0.918) ($^2\Pi$)
$^2\Pi_{1/2}$		8.78	
$^2\Sigma^+(2\sigma^1 1\pi^4)$	9.45[c]	9.19	9.19 (0.917) ($^2\Sigma^+$)
$NaBr^-$			
$X\ ^2\Sigma^+(2\sigma^2 1\pi^4 3\sigma^1)$	0.788[b]	0.68	0.68 (0.992) ($^2\Sigma^+$)

[a]Reference 83.
[b]Reference 84.
[c]Reference 85.
[d]Spin-orbit correction was added on the basis of the experimental $^2\Pi_{3/2}$ and $^2\Pi_{1/2}$ splitting in LiBr (Ref. 83).
[e]Polestrength is given in parentheses.

TABLE IV. Experimental and calculated vertical ionization potentials (IP, eV) of LiI and NaI.

Ionization transitions: $MX\ (^1\Sigma^+) \rightarrow MX^+$ or $MX^-\ (^2\Sigma^+) \rightarrow MX$	IP (exp.)	IP (theo.)[c] OVGF/TZ+*d* +diff+Corr.	IP (theo.)[d] OVGF/TZ+*d* +diff
LiI			
$X\ ^2\Pi_{3/2}(2\sigma^2 1\pi^3)$	8.44[a]	8.28	8.44 (0.926) ($^2\Pi$)
$^2\Pi_{1/2}$	8.765[a]	8.60	
$^2\Sigma^+(2\sigma^1 1\pi^4)$	9.84[a]	9.26	9.26 (0.923) ($^2\Sigma^+$)
NaI			
$X\ ^2\Pi_{3/2}(2\sigma^2 1\pi^3)$	8.80[b]	7.66	7.82 (0.931) ($^2\Pi$)
$^2\Pi_{1/2}$		7.98	
$^2\Sigma^+(2\sigma^1 1\pi^4)$	9.45[b]	8.39	8.39 (0.932) ($^2\Sigma^+$)

[a]Reference 83.
[b]Reference 85.
[c]Spin-orbit correction was added on the basis of the experimental $^2\Pi_{3/2}$ and $^2\Pi_{1/2}$ splitting in LiI (Ref. 85).
[d]Polestrength is given in parentheses.

If we average the ionization potentials (IPs) of the final $^2\Pi_{3/2}$ and $^2\Pi_{1/2}$ states for LiCl, we find that the experimental and theoretical results agree within 0.066 eV for the first IP and 0.02 eV for the second IP (Table II). The vertical EA (EAv) of LiCl is within 0.073 eV between the experiment and theory. For NaCl the calculated first and second IPs and EA agree with the experimental data within 0.14, 0.17, and 0.10 eV, respectively (Table II). The same averaging for LiBr gives 9.348 eV for the first experimental IP compared to the 9.36 eV from our calculations (Table III). The second calculated IP agrees with the experimental one within 0.17 eV. For NaBr the calculated first and second IPs and EA agree with the experimental values within 0.09, 0.26, and 0.11 eV, respectively. For LiI the calculated first IP is in good agreement with the experimental one, while the second IP is off by 0.58 eV (Table IV). For NaI the calculated first and second IPs are lower than the experimental ones by $\sim$1 eV (Table IV). We believe that the large discrepancies in the IPs of NaI and the 2σ-MO of LiI may be a result of pseudopotentials used in these calculations, or core-valent electron correlation, or relativistic effects on I. Except the latter, the overall agreement is rather good and we expect a similar agreement for small superhalogens studied here. We use the spin-orbit corrections from the diatomics in our calculations of the corresponding superhalogens, because we expect a similar order of spin-orbit contributions in the superhalogens as in the diatomics due to their similar alkali-halogen bond lengths.

IV. EXPERIMENTAL RESULTS

The experimental photoelectron spectra of LiX_2^- and NaX_2^- (X=Cl, Br, and I) are shown in Figs. 1 and 2, respectively. All the species exhibit extremely high binding energies (BEs), as expected for these superhalogens. Since no signals were observed in the low BE side, all the spectra are presented starting from 3.0 eV. We also tried to perform experiments on the corresponding fluoride superhalogens, LiF_2^- and NaF_2^-. But their electron binding energies appeared to be beyond our detachment laser photon energy (6.424 eV) and no spectra were able to be obtained. Our

Downloaded 23 May 2003 to 155.101.19.15. Redistribution subject to AIP license or copyright, see http://ojps.aip.org/jcpo/jcpcr.jsp

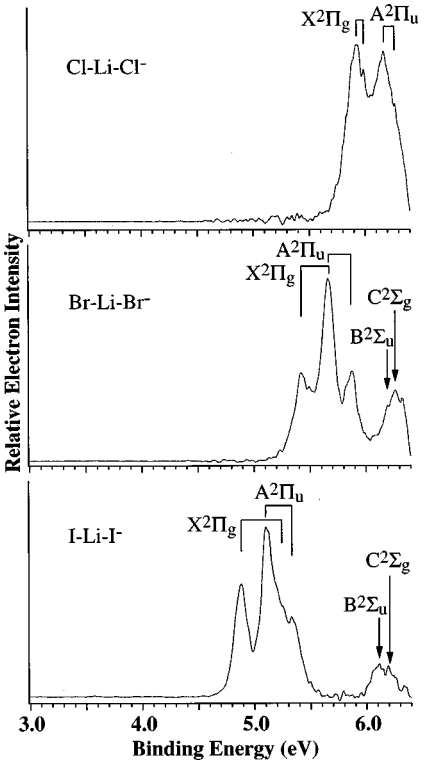

FIG. 1. Photoelectron spectra of LiX_2^- (X=Cl, Br, and I) at 193 nm. The spin-orbit splitting of the $^2\Pi$ states is indicated by the vertical lines.

inability to observe spectra of the fluoride superhalogens was also complicated by their low ion abundance due to the low solubility of the fluoride compounds in water solutions. We were able to obtain the spectrum of KF_2^-, whose VDE was measured to be 5.61 ± 0.04 eV. However, in this paper, we only focus on the Li- and Na-containing species. Overall, we found that the BEs of the MX_2^- species decrease as the size of the metal and halogen ions increases, as expected from the simple electrostatic argument. For the Br- and I-containing species, we observed more spectral features, which also exhibit obvious similarities for the same metal (Figs. 1 and 2). The measured VDEs for the spectral features are summarized in Tables VI–VIII, for the Cl-, Br-, and I-containing species, respectively. The detailed assignment and comparisons with the theoretical calculations will be discussed for each superhalogen in the following section.

V. SPECTRAL ASSIGNMENTS AND DISCUSSION

In previous studies[4,5,16,23,33] it was found that all the MX_2^- anions have a linear structure and can be viewed as simple $X^{-1}M^{+1}X^{-1}$ ionic systems as expected. Their valence electronic configurations can be described as $1\sigma_g^2 1\sigma_u^2 2\sigma_g^2 2\sigma_u^2 1\pi_u^4 1\pi_g^4$, where $1\sigma_g$ and $1\sigma_u$ are mainly the bonding and antibonding MOs from the *s* valence orbitals of the halogens; $2\sigma_g$ and $1\pi_u$, and $2\sigma_u$ and $1\pi_g$ are the bonding and antibonding MOs from the valence *p* orbitals of the halogens. A similar picture was found for all the MX_2^- superhalogens in this study as well. The results of our calculations for $LiCl_2^-$, $NaCl_2^-$, $LiBr_2^-$, $NaBr_2^-$, LiI_2^-, and NaI_2^- are presented in Table V. For $LiCl_2^-$ and $NaCl_2^-$ our results are in excellent agreement with previous calculations at the B3LYP/6-311+G*, MBPT2/6-311+G* and CCSD/6-311+G* level of theory[33] and at the configuration interaction with single and double excitations (CISD) level of theory using TZP+SP diffuse functions basis sets.[23] For the remaining four anions containing Br and I, there were no previous studies and thus calculations have been performed for the first time. Optimized geometries for the anions were then used to calculate VDEs to help the interpretation of the obtained experimental photoelectron spectra. Previous calculations found that the equilibrium geometries of the neutral superhalogens, $LiCl_2$ and $NaCl_2$, are not linear, but bent with rather small bond angles. Calculations on the neutral species are more challenging, and we did not perform further calculations on them. Since photodetachment processes by nature are vertical processes, we found that the calculations on the anions and the calculated VDEs are adequate to interpret the experimental data.

Photodetachment is expected to take place from the valence MOs in each anion ($1\sigma_g^2 1\sigma_u^2 2\sigma_g^2 2\sigma_u^2 1\pi_u^4 1\pi_g^4$). Depending on their binding energies, detachment from all or only the top few MOs may be observed experimentally. Even though the spacing among the MOs was expected to be different for each species, similar spectral features were expected to be observed. Furthermore, detachment from the two π orbitals should result in two spin-orbit components, complicating the spectral assignments. Large spin-orbit splitting should be observed in the Br- and I-containing species and the systematic study here helps their identification together with the theoretical calculations.

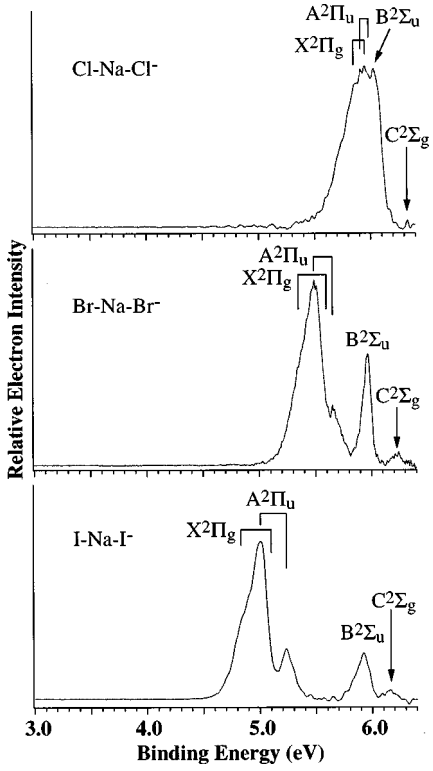

FIG. 2. Photoelectron spectra of NaX_2^- (X=Cl, Br, and I) at 193 nm. The spin-orbit splitting of the $^2\Pi$ states is indicated by the vertical lines.

Downloaded 23 May 2003 to 155.101.19.15. Redistribution subject to AIP license or copyright, see http://ojps.aip.org/jcpo/jcpcr.jsp

TABLE V. Calculated molecular properties of $LiCl_2^-$, $NaCl_2^-$, $LiBr_2^-$, $NaBr_2^-$, LiI_2^-, and NaI_2^-.

Molecule ($D_{\infty h}$, $^1\Sigma_g^+$)	$E_{CCSD(T)}$ (a.u.)	R (M-X) (Å)	$\nu_1(\sigma_g)$ (cm^{-1})	$\nu_2(\sigma_u)$ (cm^{-1})	$\nu_3(\pi_u)$ (cm^{-1})	ZPE[c] (eV)
$LiCl_2^-$[a]	−927.019 970	2.140	220	688	177	0.078
$NaCl_2^-$[a]	−1081.396 675	2.492	191	366	90	0.046
$LiBr_2^-$[a]	−5152.723 228	2.316	132	603	148	0.064
$NaBr_2^-$[a]	−5307.106 325	2.662	116	307	71	0.035
LiI_2^-[b]	−30.182 789	2.507				
NaI_2^-[b]	−22.902 980	2.874				

[a]CCSD(T)/6–311+G*.
[b]CCSD(T)/TZ+*d*+diff.
[c]Zero point energy.

A. $LiCl_2^-$ and $NaCl_2^-$

The photoelectron spectrum of $LiCl_2^-$ (Fig. 1) showed two major peaks with very high VDEs at 5.92 and 6.17 eV, respectively. Other fine features are discernible as shown in Fig. 1. Without spin-orbit corrections our calculations showed four electron detachment transitions. The VDEs of the first two transitions, due to detachment from the π_g and π_u MOs ($^2\Pi_g$ and $^2\Pi_u$ final states), are found to be very close to each other; the other two transitions due to detachment from the $2\sigma_u$ and $2\sigma_g$ MOs ($^2\Sigma_u^+$ and $^2\Sigma_g^+$ final states) are separated from the first group by 0.43 eV (Table VI). These results are consistent with the theoretical (0.60 eV) and experimental (0.69 eV) $^2\Pi$-$^2\Sigma^+$ splitting in LiCl (Table II). The VDEs of the transitions to the $^2\Sigma_g^+$ and $^2\Sigma_u^+$ final states (6.52 and 6.8 eV) are beyond our photon energy (6.424 eV). Therefore, the two observed major spectral features are assigned to be from detachment of the two π MOs of $LiCl_2^-$. When spin-orbit corrections were added, the calculated VDEs are again separated into two groups of peaks with the first group almost equidistantly covering the BE range from 5.90 to 6.12 eV. The 0.06 eV spin-orbit splitting for the two $^2\Pi$ states is quite close to the ν_2 vibrational frequency of the anion, complicating the assignments of the fine features in the spectrum of $LiCl_2^-$. We tentatively assign the fine features to the spin-orbit splitting. As seen from Table VI, the agreement between the calculated and measured VDEs for the $^2\Pi_g$ states is excellent, although the agreement is less than ideal for the $^2\Pi_u$ states.

The spectrum of $NaCl_2^-$ (Fig. 2) is more congested and complicated. Several features can be identified in the broad and strong band from 5.6–6.1 eV. A very weak, but well resolved peak is also observed at 6.33 eV. The measured VDEs for the observed features are summarized in Table VI, along with those of $LiCl_2^-$ and compared to the calculated results. Without spin-orbit corrections our calculations yielded four electron detachment transitions with the first two transitions ($^2\Pi_g$ and $^2\Pi_u$ final states) being very close to each other (within 0.03 eV) and two others transitions ($^2\Sigma_g$ and $^2\Sigma_u^+$ final states) being separated from the first group by 0.19 eV. In the NaCl photoelectron spectrum the $^2\Pi$-$^2\Sigma^+$ splitting is 0.46 ± 0.08 eV (Table II), which is smaller than that in LiCl. Therefore, the smaller $^2\Pi$-$^2\Sigma^+$ splitting in $NaCl_2^-$ than that in $LiCl_2^-$ is consistent with the trend in the diatomics. When spin-orbit corrections were added, the calculated VDEs are again separated into two groups of peaks with the first group almost equidistantly covering the BE

TABLE VI. Experimental and calculated vertical detachment energies (VDE, eV) of $ClLiCl^-$ and $ClNaCl^-$.

Detachment transitions: $ClMCl^-$ ($^1\Sigma_g^+$)→ClMCl	VDE (exp.)[a]	VDE (theo.)[b] OVGF/6–311+ G(2*df*)+Corr.	VDE (theo.)[c] OVGF/6–311+ G(2*df*)
ClLiCl			
X $^2\Pi_{g3/2}$ ($2\sigma_g^2 2\sigma_u^2 1\pi_u^4 1\pi_g^3$)	5.92 (4)	5.90	5.93 (0.913) ($^2\Pi_g$)
$^2\Pi_{g1/2}$	5.99 (4)	5.96	
A $^2\Pi_{u3/2}$ ($2\sigma_g^2 2\sigma_u^2 1\pi_u^3 1\pi_g^4$)	6.17 (4)	6.06	6.09 (0.915) ($^2\Pi_u$)
$^2\Pi_{u1/2}$	6.27 (4)	6.12	
B $^2\Sigma_u^+$ ($2\sigma_g^2 2\sigma_u^1 1\pi_u^4 1\pi_g^4$)		6.52	6.52 (0.914) ($^2\Sigma_u^+$)
C $^2\Sigma_g^+$ ($2\sigma_g^1 2\sigma_u^2 1\pi_u^4 1\pi_g^4$)		6.58	6.58 (0.912) ($^2\Sigma_g^+$)
ClNaCl			
X $^2\Pi_{g3/2}$ ($2\sigma_g^2 2\sigma_u^2 1\pi_u^4 1\pi_g^3$)	5.86 (6)	5.81	5.84 (0.914) ($^2\Pi_g$)
A $^2\Pi_{u3/2}$ ($2\sigma_g^2 2\sigma_u^2 1\pi_u^3 1\pi_g^4$)	5.91 (6)	5.84	5.87 (0.915) ($^2\Pi_u$)
$^2\Pi_{g1/2}$	5.95 (6)	5.87	
$^2\Pi_{u1/2}$	5.98 (6)	5.90	
B $^2\Sigma_u^+$ ($2\sigma_g^2 2\sigma_u^1 1\pi_u^4 1\pi_g^4$)	6.03 (4)	6.06	6.06 (0.913) ($^2\Sigma_u^+$)
C $^2\Sigma_g^+$ ($2\sigma_g^1 2\sigma_u^2 1\pi_u^4 1\pi_g^4$)	6.33 (3)	6.35	6.35 (0.915) ($^2\Sigma_g^+$)

[a]The number in the parentheses is the uncertainty in the last digit.
[b]Spin-orbit correction was made based on the $^2\Pi_{3/2}$-$^2\Pi_{1/2}$ splitting (0.060 eV) in LiCl.
[c]Polestrength is given in parentheses.

Downloaded 23 May 2003 to 155.101.19.15. Redistribution subject to AIP license or copyright, see http://ojps.aip.org/jcpo/jcpcr.jsp

TABLE VII. Experimental and calculated vertical detachment energies (VDE, eV) of $BrLiBr^-$ and $BrNaBr^-$.

Detachment transitions: $BrMBr^-$ ($^1\Sigma_g^+$)→BrMBr	VDE (exp.)[a]	VDE (theo.)[b] OVGF/6–311+ G(2*df*)+Corr.	VDE (theo.)[c] OVGF/6–311+ G(2*df*)
BrLiBr			
$X\ ^2\Pi_{g3/2}(2\sigma_g^2 2\sigma_u^2 1\pi_u^4 1\pi_g^3)$	5.42 (3)	5.48	5.58 (0.915) ($^2\Pi_g$)
$A\ ^2\Pi_{u3/2}(2\sigma_g^2 2\sigma_u^2 1\pi_u^3 1\pi_g^4)$	5.66 (6)	5.62	5.72 (0.916) ($^2\Pi_u$)
$^2\Pi_{g1/2}$	5.66 (6)	5.68	
$^2\Pi_{u1/2}$	5.88 (3)	5.82	
$B\ ^2\Sigma_u^+(2\sigma_g^2 2\sigma_u^1 1\pi_u^4 1\pi_g^4)$	6.19 (3)	6.19	6.19 (0.913) ($^2\Sigma_u^+$)
$C\ ^2\Sigma_g^+(2\sigma_g^1 2\sigma_u^2 1\pi_u^4 1\pi_g^4)$	6.26 (3)	6.22	6.22 (0.915) ($^2\Sigma_g^+$)
BrNaBr			
$X\ ^2\Pi_{g3/2}(2\sigma_g^2 2\sigma_u^2 1\pi_u^4 1\pi_g^3)$	5.36 (6)	5.42	5.52 (0.915) ($^2\Pi_g$)
$A\ ^2\Pi_{u3/2}(2\sigma_g^2 2\sigma_u^2 1\pi_u^3 1\pi_g^4)$	5.49 (4)	5.46	5.56 (0.916) ($^2\Pi_u$)
$^2\Pi_{g1/2}$	5.60 (6)	5.62	
$^2\Pi_{u1/2}$	5.65 (3)	5.66	
$B\ ^2\Sigma_u^+(2\sigma_g^2 2\sigma_u^1 1\pi_u^4 1\pi_g^4)$	5.96 (3)	5.76	5.76 (0.914) ($^2\Sigma_u^+$)
$C\ ^2\Sigma_g^+(2\sigma_g^1 2\sigma_u^2 1\pi_u^4 1\pi_g^4)$	6.21 (4)	6.06	6.06 (0.916) ($^2\Sigma_g^+$)

[a]The number in the parentheses is the uncertainty in the last digit.
[b]Spin-orbit correction was made based on the $^2\Pi_{3/2}$-$^2\Pi_{1/2}$ splitting (0.213 eV) in LiBr.
[c]Polestrength is given in parentheses.

range from 5.81 to 6.06 eV and one state occurs at 6.35 eV. The close spacing among the first group of states, $^2\Pi_{g3/2}$, $^2\Pi_{u3/2}$, $^2\Pi_{g1/2}$, $^2\Pi_{u1/2}$, and $^2\Sigma_u$, is perfectly consistent with the observed broad peak from 5.6–6.1 eV and are assigned accordingly as shown in Fig. 2. The measured VDE of the weak peak at 6.33 eV is in excellent agreement with the calculated VDE of the $^2\Sigma_g$ state. The overall assignments are shown in Fig. 2 and Table VI. The measured and calculated VDEs agree very well. The cross section for detachment of the $2\sigma_g$ MO ($^2\Sigma_g$ final state) appeared to be unusually low. As we will see in the following, this is also the case for $NaBr_2^-$ and NaI_2^- (see Fig. 2).

The first VDEs reported in Table VI for $LiCl_2^-$ and $NaCl_2^-$ were calculated by the so-called direct method, in which electron correlation and electron relaxation corrections calculated within the OVGF technique were added to the energy of the highest occupied molecular orbital (HOMO). Our results can be compared with the similar, but somewhat more accurate, third-order algebraic diagrammatic contraction Green function [ADC (3)] method, which Scheller and Cederbaum[23] used to calculate the same VDEs employing the TZ+*d*+diff basis sets. Their VDEs were found to be 5.73 eV ($LiCl_2^-$) and 5.64 eV ($NaCl_2^-$), which are very close to the values calculated here.[78] VDEs can also be calculated using the so-called indirect method, where they are evaluated as the energy difference between the total energy of the anion and that of its neutral precursor at the optimal geometry of the anion. Gutsev and others performed such calculation[33]

TABLE VIII. Experimental and calculated vertical detachment energies (VDE, eV) of $ILiI^-$ and $INaI^-$.

Detachment transitions: IMI^- ($^1\Sigma_g^+$)→IMI	VDE (exp.)[a]	VDE (theo.)[b] OVGF/TZ+*d* +diff+Corr.	VDE (theo.)[c] OVGF/TZ+*d* +diff
ILiI			
$X\ ^2\Pi_{g3/2}(2\sigma_g^2 2\sigma_u^2 1\pi_u^4 1\pi_g^3)$	4.88 (3)	4.57	4.73 (0.945) ($^2\Pi_g$)
$A\ ^2\Pi_{u3/2}(2\sigma_g^2 2\sigma_u^2 1\pi_u^3 1\pi_g^4)$	5.10 (3)	4.83	4.99 (0.928) ($^2\Pi_u$)
$^2\Pi_{g1/2}$	5.24 (6)	4.90	
$^2\Pi_{u1/2}$	5.33 (3)	5.15	
$B\ ^2\Sigma_u^+(2\sigma_g^2 2\sigma_u^1 1\pi_u^4 1\pi_g^4)$	6.11 (4)	5.93[d]	5.35 (0.941) ($^2\Sigma_u^+$)
$C\ ^2\Sigma_g^+(2\sigma_g^1 2\sigma_u^2 1\pi_u^4 1\pi_g^4)$	6.20 (4)	6.54[d]	5.96 (0.923) ($^2\Sigma_g^+$)
INaI			
$X\ ^2\Pi_{g3/2}(2\sigma_g^2 2\sigma_u^2 1\pi_u^4 1\pi_g^3)$	4.84 (6)	4.50	4.67 (0.954) ($^2\Pi_g$)
$A\ ^2\Pi_{u3/2}(2\sigma_g^2 2\sigma_u^2 1\pi_u^3 1\pi_g^4)$	5.01 (4)	4.75	4.91 (0.922) ($^2\Pi_u$)
$^2\Pi_{g1/2}$	5.10 (6)	4.84	
$^2\Pi_{u1/2}$	5.23 (3)	5.08	
$B\ ^2\Sigma_u^+(2\sigma_g^2 2\sigma_u^1 1\pi_u^4 1\pi_g^4)$	5.92 (3)	6.07[e]	5.01 (0.942) ($^2\Sigma_u^+$)
$C\ ^2\Sigma_g^+(2\sigma_g^1 2\sigma_u^2 1\pi_u^4 1\pi_g^4)$	6.16 (4)	6.49[e]	5.43 (0.930) ($^2\Sigma_g^+$)

[a]The number in the parentheses is the uncertainty in the last digit.
[b]Spin-orbit correction was made based on the $^2\Pi_{3/2}$-$^2\Pi_{1/2}$ splitting (0.33 eV) in LiI.
[c]Polestrength is given in parentheses.
[d]An empirical correction of 0.58 eV was added to the $^2\Sigma^+$-type states based on the LiI results (see Table III).
[e]An empirical correction of 1.06 eV was added to the $^2\Sigma^+$-type states based on the NaI results (see Table III).

Downloaded 23 May 2003 to 155.101.19.15. Redistribution subject to AIP license or copyright, see http://ojps.aip.org/jcpo/jcpcr.jsp

at the CCSD(T) level of theory employing large Widmark–Malmquist–Roos (WMR) basis sets. Their VDEs were found to be 5.88 eV ($LiCl_2^-$) and 5.77 eV ($NaCl_2^-$), which are again in excellent agreement with the results of this work.

B. $LiBr_2^-$ and $NaBr_2^-$

The photoelectron spectrum of $LiBr_2^-$ is shown in Fig. 1. Three well-resolved features are observed at 5.42, 5.66, and 5.88 eV, followed by a broadband at high BE with fine features. The measured VDEs are listed in Table VII, along with the calculated results. Without spin-orbit corrections we found four detachment transitions from the calculations. The first two transitions from the π_g and π_u MOs ($^2\Pi_g$ and $^2\Pi_u$ final states) are found to be very close to each other; the other two transitions from the $2\sigma_u$ and $2\sigma_g$ MOs ($^2\Sigma_u^+$ and $^2\Sigma_g^+$ final states) are separated from the first group by 0.47 eV. The slightly larger $^2\Pi$-$^2\Sigma^+$ splitting in $LiBr_2^-$ compared to that in $LiCl_2^-$ is consistent with the larger $^2\Pi$-$^2\Sigma^+$ splitting in LiBr (0.86 eV) compared to that in LiCl (0.68 eV) (see Tables II and III). One may expect a more profound effect of spin-orbit coupling for this anion relative to that in $LiCl_2^-$. When the spin-orbit corrections were included, the $^2\Pi_{g3/2}$ state was found to be separated by 0.20 eV from the $^2\Pi_{g1/2}$ state. A similar spin-orbit splitting was found for $^2\Pi_{u3/2}$ and $^2\Pi_{u1/2}$. Interestingly, the $^2\Pi_{u3/2}$ and $^2\Pi_{g1/2}$ spin-orbit states are now becoming very close to each other in energy. This calculated energy level structure is pleasingly consistent with the observed spectrum of $LiBr_2^-$. There are three main features below 6.0 eV with the middle one being almost twice more intense than its neighbors, suggesting that the intense feature may actually have contributions from two overlapping states. The assignments of the four spin-orbit states are shown in Fig. 1. The VDEs for the two detachment transitions from the $2\sigma_u$ and $2\sigma_g$ MOs are calculated to be very close to each other (within 0.03 eV), suggesting that they would overlap with each other and yield the broad feature near 6.2 eV. Additional fine features discernible in the spectrum of $LiBr_2^-$ are likely to be due to vibrational fine structures. Overall the agreement between the measured and calculated VDEs for $LiBr_2^-$ is excellent.

The spectrum of $NaBr_2^-$ is shown in Fig. 2. Five features can be easily identified with the ground state feature showing as a shoulder near 5.36 eV. The two high BE features are well resolved with the highest BE feature being very weak. The VDEs are listed in Table VII, together with that of $LiBr_2^-$ and the calculated results. Compared to that of $NaCl_2^-$, the assignment of the features in $NaBr_2^-$ is straightforward. Without spin-orbit corrections we found four detachment transitions with the first two transitions ($^2\Pi_g$ and $^2\Pi_u$ final states) being very close to each other. There is one transition ($^2\Sigma_u^+$ final state) being separated from the first group by 0.20 eV and another ($^2\Sigma_g^+$ final state) being separated from the third by 0.30 eV. When spin-orbit corrections were added to the calculated VDEs, the $^2\Pi_g$ and $^2\Pi_u$ final states were found to each split into two spin-orbit components separated by 0.20 eV. The overall assignments are shown in Fig. 2. From Table VII we see that the agreement between the measured and calculated VDEs is very good except the ground state feature. The latter is likely due to the fact that the ground state feature was observed as a shoulder and its VDE was difficult to be accurately determined.

C. LiI_2^- and NaI_2^-

The photoelectron spectrum of LiI_2^- is shown in Fig. 1. It is very similar to that of $LiBr_2^-$. The measured VDEs are listed in Table VIII and compared to the calculated results. In LiI the $^2\Pi$-$^2\Sigma^+$ splitting is very high (1.06 eV, Table IV) and one expects a large $^2\Pi$-$^2\Sigma^+$ splitting in LiI_2^-. Indeed, the spectrum of LiI_2^- displays two groups of peaks. One group at lower BE (4.8–5.4 eV) is well separated from another group at higher BE around 6.1 eV. The assignments of these features are straightforward by comparing to that of $LiBr_2^-$. As we already discussed above, our calculated IP from the 2σ MO of LiI was heavily underestimated. Therefore, in addition to spin-orbit corrections, we added an empirical correction (estimated from LiI) to all VDEs of the $^2\Sigma^+$ symmetry. After all corrections were added, the spin-orbit state ($^2\Pi_{g3/2}$) was found to be separated by 0.26 eV from the group of two states ($^2\Pi_{u3/2}$ and $^2\Pi_{g1/2}$), which are very close to each other. The $^2\Pi_{u1/2}$ state was separated from the $^2\Pi_{g1/2}$ state by 0.25 eV. The states of $^2\Sigma^+$ symmetry are well separated from those of the $^2\Pi$ symmetry. This energy level picture is consistent with the observed spectrum of LiI_2^-. The overall assignments are given in Fig. 1. As seen from Table VIII, the calculated VDEs are systematically lower than the measured values. But the trends are consistent, except the separation between the two $^2\Sigma^+$ states. The measured separation is rather small, whereas the calculations predicted a much larger value. The small measured separation is consistent with that observed in $LiBr_2^-$. However, these features were not well experimentally resolved and thus their VDEs can only be tentatively assigned. On the other hand, the calculations are also less accurate and more accurate calculations are probably needed to resolve this.

The spectrum of NaI_2^- is shown in Fig. 2 and exhibits obvious similarities to that of $NaBr_2^-$. The VDEs of the observed features are listed in Table VIII along with the calculated results. Similar spectral assignments can be made based on those of the $NaBr_2^-$. Without spin-orbit corrections we found four detachment transitions with the first two transitions ($^2\Pi_g$ and $^2\Pi_u$ final states) being very close to each other, one transition ($^2\Sigma_u^+$ final state) being separated from the first group by 0.20 eV and another one ($^2\Sigma_g^+$ final state) being separated from the third by 0.30 eV. In NaI the $^2\Pi$-$^2\Sigma^+$ splitting is 0.65 eV (Table IV) and one can expect that transitions to the $^2\Pi$ and $^2\Sigma^+$ states in NaI_2^- should also be well separated. This was indeed what we found in our calculations and in the experimental spectrum. All the assignments are given in Fig. 2. Again the calculated VDEs are consistent with the measured values, but quantitative agreement is not achieved, as shown in Table VIII. We would like to stress here, that because of the use of pseudopotentials and the absence of relativistic effects in our calculations of iodine-containing molecules, these results should be considered as rather crude and more quantitative analysis of these spectra will require further calculations.

Downloaded 23 May 2003 to 155.101.19.15. Redistribution subject to AIP license or copyright, see http://ojps.aip.org/jcpo/jcpcr.jsp

D. Overview and discussion

The largest experimentally measured VDE was for $LiCl_2^-$ (5.92 ± 0.04 eV). The VDEs were found to decrease in the series: $LiCl_2^-$ (5.92 eV)$\rightarrow$$NaCl_2^-$ (5.86 eV) $\rightarrow$ $LiBr_2^-$ (5.42 eV) $\rightarrow$ $NaBr_2^-$ (5.36 eV) $\rightarrow$ LiI_2^- (4.88 eV) $\rightarrow$ NaI_2^- (4.84 eV). All six measured VDEs are extremely high and much larger than 3.61 eV (the largest VDE for the halogen anions). According to this trend, LiF_2^- should possess the highest VDE among the MX_2^- superhalogens. Indeed, we were not able to observe photodetachment from this anion with our 6.424 eV photon energy, consistent with the previous calculated VDE of 6.51 eV for this anion.[33] The VDE of NaF_2^- was calculated to be 6.18 eV previously.[33] However, we failed to observe detachment from this anion either, probably due to the weak mass signals (the fluorides tend to have very low solubility in the water solution). The only fluoride superhalogen from which we were able to observe detachment was KF_2^-, which has a VDE of 5.61 ± 0.04 eV. This suggests that a previously calculated VDE for KF_2^- (6.07 eV) was too high.[23]

Besides the above trend in VDEs among the superhalogens, the photoelectron spectra shown in Figs. 1 and 2 reveal several other trends which shed light on the chemical bonding properties of the MX_2^- superhalogens. First, we observed that the separation between the π-type and σ-type orbitals increases as the size of the halogen ions increases for both the LiX_2^- and NaX_2^- series. This trend is similar to that observed in the diatomics. Comparing the spectra in Fig. 1 and 2, two other interesting trends are evident: the spacing between the π_g and π_u MOs is larger in the LiX_2^- series than that in the NaX_2^- series, whereas the separation between the σ_u and σ_g MOs is the opposite. It is larger in the NaX_2^- series than that in the LiX_2^- series. This observation suggests that the $p_\pi - p_\pi$ interactions in the LiX_2^- series are more important than the $p_\sigma - p_\sigma$ interactions, probably due to the smaller size of the Li^+ ion. On the other hand, the $p_\sigma - p_\sigma$ interactions are more important than the $p_\pi - p_\pi$ interactions in the NaX_2^- series. Furthermore, we observed that at the current detachment photon energy all the π-type MOs seem to have higher detachment cross sections than those of the σ type. In particular, we found that detachment cross section for the $2\sigma_g$ MO in the NaX_2^- series is unusually low, as seen clearly from Fig. 2.

The reason that the VDE is substantially higher for the MX_{k+1}^- superhalogens than those for X^- has already been briefly discussed on the basis of the DVM-X_α calculations.[4,33] Four main reasons have been pointed out in Refs. 4 and 33 as being responsible for the increase of VDE in LiF_2^- relative to F^-: (1) delocalization of the extra electron over two fluorine atoms instead of one; (2) nonbonding character of the HOMO [central atom does not contribute valence atomic orbitals (AOs) to the HOMO] and therefore the HOMO is composed entirely of the p_π-AOs of the highly electronegative fluorine atoms; (3) coordination of F^- anion to the electropositive ion Li^+, i.e., electrostatic effect; (4) electron relaxation and electron correlation effects.

The same order of excited states as considered here for the superhalogens was found by Ortiz for another type of superhalogens, BO_2^-,[24] and BS_2^-,[25] which are in fact valence isoelectronic to the anions studied here. Ortiz used the *ab initio* electron propagator method with 6-311+G($2df$) basis sets.[79] Both of these anions were found to have very high VDEs: 4.75 eV (BO_2^-) and 3.68 eV (BS_2^-), while all of the superhalogen anions studied here possess even higher VDEs.

In all electron detachment processes considered here we found that the polestrengths are very high (close to 1.0, see Tables VI–VIII), which means that all the electron detachment processes can be considered as essentially one-electron processes.

VI. CONCLUSIONS

We reported a combined photoelectron spectroscopic and theoretical study of six superhalogen anions, MX_2^- (M=Li and Na; X=Cl, Br, and I). For the first time, the extremely high electron detachment energies from the superhalogens were verified experimentally. We anticipate that progress in developing even more powerful lasers and the ESI technique will help study superhalogens with EAs up to the current theoretical limit of 12–14 eV.[80,81] Superhalogens with such exceptionally high EAs may be used to attempt to make a chemically bound species of argon, yet to be synthesized. They may also be useful for the synthesis of other new energy rich materials.

ACKNOWLEDGMENTS

The theoretical work done in Utah is supported by the National Science Foundation (CHE-9618904). The authors wish to thank Dr. V. G. Zarkzewski for fruitful discussion of the OVGF results in this work. The experimental work done at Pacific Northwest National Laboratory is supported by the U.S. Department of Energy, Office of Basic Energy Sciences, Chemical Science Division. L.S.W. wishes to thank the Donors of the Petroleum Research Fund, administered by the American Chemical Society, for partial support of this research. PNNL is operated by Battelle for the DOE under Contract No. DE-AC06-76RLO 1830. L.S.W. is an Alfred P. Sloan Research Fellow.

[1] N. Bartlett, Proc. Chem. Soc. 218 (1962).
[2] F. Wudl, Acc. Chem. Res. **17**, 227 (1984).
[3] H. Hotop and W. C. Lineberger, J. Phys. Chem. Ref. Data **14**, 731 (1985).
[4] G. L. Gutsev and A. I. Boldyrev, Chem. Phys. **56**, 277 (1981).
[5] G. L. Gutsev and A. I. Boldyrev, Adv. Chem. Phys. **61**, 169 (1985).
[6] P. J. Hay, W. R. Wadt, L. R. Kahn, R. C. Raffenetti, and D. H. Phillips, J. Chem. Phys. **71**, 1767 (1979).
[7] J. E. Bloor and R. E. Sherrod, J. Am. Chem. Soc. **102**, 4333 (1980).
[8] G. L. Gutsev and A. I. Boldyrev, Chem. Phys. Lett. **84**, 352 (1981).
[9] G. L. Gutsev and A. I. Boldyrev, Chem. Phys. Lett. **101**, 441 (1983).
[10] G. L. Gutsev and A. I. Boldyrev, Chem. Phys. **108**, 250 (1984).
[11] G. L. Gutsev and A. I. Boldyrev, Chem. Phys. **108**, 254 (1984).
[12] G. L. Gutsev and A. I. Boldyrev, Mol. Phys. **53**, 23 (1984).
[13] Y. Sakai and E. Miyoshi, J. Chem. Phys. **87**, 2885 (1987).
[14] E. Miyoshi, Y. Sakai, A. Murakami, H. Iwaki, H. Terashima, T. Shoda, and T. Kawaguchi, J. Chem. Phys. **89**, 4193 (1988).
[15] F. Mota, J. J. Novoa, and A. C. Ramirez, J. Mol. Struct.: THEOCHEM **43**, 153 (1988).
[16] V. G. Zakzhevskii and A. I. Boldyrev, J. Chem. Phys. **93**, 657 (1990).

Downloaded 23 May 2003 to 155.101.19.15. Redistribution subject to AIP license or copyright, see http://ojps.aip.org/jcpo/jcpcr.jsp

[17] C. Komel, G. Palm, R. Ahlrichs, M. Bar, and A. I. Boldyrev, Chem. Phys. Lett. **173**, 151 (1990).
[18] A. I. Boldyrev and W. von Niessen, Chem. Phys. **155**, 71 (1991).
[19] H.-G. Weikert, L. S. Cederbaum, F. Tarantelli, and A. I. Boldyrev, Z. Phys. D **18**, 299 (1991).
[20] G. L. Gutsev, Chem. Phys. Lett. **184**, 305 (1991).
[21] M. K. Scheller and L. S. Cederbaum, J. Phys. B **25**, 2257 (1992).
[22] A. I. Boldyrev and J. Simons, J. Chem. Phys. **97**, 2826 (1992).
[23] M. K. Scheller and L. S. Cederbaum, J. Chem. Phys. **99**, 441 (1993).
[24] J. V. Ortiz, J. Chem. Phys. **99**, 6727 (1993).
[25] J. V. Ortiz, Chem. Phys. Lett. **214**, 467 (1993).
[26] H.-G. Weikert and L. S. Cederbaum, J. Chem. Phys. **99**, 8877 (1993).
[27] G. L. Gutsev, J. Chem. Phys. **98**, 444 (1993).
[28] G. L. Gutsev, J. Chem. Phys. **99**, 3906 (1993).
[29] M. K. Scheller and L. S. Cederbaum, J. Chem. Phys. **100**, 8934 (1994).
[30] G. L. Gutsev, A. Les, and L. Adamowicz, J. Chem. Phys. **100**, 8925 (1994).
[31] H.-G. Weikert, H.-D. Meyer, and L. S. Cederbaum, J. Chem. Phys. **104**, 7122 (1996).
[32] M. Gutowski, A. I. Boldyrev, J. Simons, J. Raz, and J. Blazejowski, J. Am. Chem. Soc. **118**, 1173 (1996).
[33] G. L. Gutsev, R. J. Bartlett, A. I. Boldyrev, and J. Simons, J. Chem. Phys. **107**, 3867 (1997).
[34] G. L. Gutsev, P. Jena, and R. J. Bartlett, Chem. Phys. Lett. **292**, 289 (1998).
[35] N. Bartlett, Angew. Chem. Int. Ed. Engl. **7**, 433 (1968).
[36] D. E. Jensen, Trans. Faraday Soc. **65**, 2123 (1969).
[37] D. E. Jensen and W. J. Miller, J. Chem. Phys. **53**, 3287 (1970).
[38] E. E. Ferguson, D. B. Dunkin, and F. C. Feshenfeld, J. Chem. Phys. **57**, 1459 (1972).
[39] W. J. Miller, J. Chem. Phys. **57**, 2354 (1972).
[40] J. Burgess, I. H. Haigh, R. D. Peacock, and P. Taylor, J. Chem. Soc. Dalton Trans. **10**, 1064 (1974).
[41] C. B. Leffert, S. Y. Tang, E. W. Rothe, and T. C. Cheng, J. Chem. Phys. **61**, 4929 (1974).
[42] J. Burgess, I. H. Haigh, R. D. Peacock, and P. Taylor, J. Chem. Soc. (Dalton) 1064 (1974).
[43] C. D. Cooper and R. N. Compton, Bull. Am. Phys. Soc. **19**, 1067 (1974).
[44] S. Y. Tang, G. P. Reck, and E. W. Rothe, Bull. Am. Phys. Soc. **19**, 1173 (1974).
[45] M. Boring, J. H. Wood, and J. W. Moskowtiz, J. Chem. Phys. **61**, 3800 (1974).
[46] R. K. Gould and W. J. Miller, J. Chem. Phys. **62**, 644 (1975).
[47] J. L. Beauchamp, J. Chem. Phys. **64**, 929 (1976).
[48] B. P. Mathur, E. W. Rothe, S. Y. Tang, and K. Mahajan, J. Chem. Phys. **64**, 1247 (1976).
[49] R. N. Compton, J. Chem. Phys. **66**, 4478 (1977).
[50] B. P. Mathur, E. W. Rothe, and G. P. Reck, J. Chem. Phys. **67**, 377 (1977).
[51] R. N. Compton, P. W. Reinhart, and C. D. Cooper, J. Chem. Phys. **68**, 2023 (1978).
[52] A. T. Pyatenko and L. N. Gorokhov, Chem. Phys. Lett. **105**, 205 (1984).
[53] R. N. Compton, in *Photophysics and Photochemistry in the Vacuum Ultraviolet*, NATO ASI Series C: Mathematical and Physical Sciences, Vol. 142, edited by S. P. McGlynn, C. L. Findley, and R. A. Huebner (Reidel, Boston, 1985), p. 261.
[54] N. A. Igolkina, M. I. Nikitin, O. V. Boltalina, and L. V. Sidorov, High. Temp. Sci. **21**, 111 (1986).
[55] N. A. Igolkina, M. I. Nikitin, L. V. Sidorov, and O. V. Boltalina, High. Temp. Sci. **23**, 89 (1987).
[56] A. Ya. Borshchevskii, O. V. Boltalina, I. D. Sorokin, and L. N. Sidorov, J. Chem. Thermodyn. **20**, 523 (1988).
[57] L. N. Sidorov, O. V. Boltalina, and A. Ya. Borshchevski, Int. J. Mass Spectrom. Ion Processes **87**, R1 (1989).
[58] O. V. Boltalina, A. Ya. Borshchevskii, and L. V. Sidorov, Russ. J. Phys. Chem. **65**, 466 (1991).
[59] R. N. Compton, in *Negative Ions*, edited by V. A. Esaulov (Cambridge University Press, Cambridge, 1995).
[60] L. S. Wang, C. F. Ding, X. B. Wang, and S. E. Barlow, Rev. Sci. Instrum. (in press).
[61] X. B. Wang, C. F. Ding, and L. S. Wang, Phys. Rev. Lett. **81**, 3351 (1998).
[62] L. S. Wang, C. F. Ding, X. B. Wang, and J. B. Nicholas, Phys. Rev. Lett. **81**, 2667 (1998).
[63] C. F. Ding, X. B. Wang, and L. S. Wang, J. Phys. Chem. A **102**, 8633 (1998).
[64] G. D. Purvis, III and R. J. Bartlett, J. Chem. Phys. **76**, 1910 (1982).
[65] M. Urban, J. Noga, S. L. Cole, and J. Bartlett, J. Chem. Phys. **83**, 4041 (1985).
[66] GAUSSIAN 94 (revision A.1). M. J. Frisch, G. M. Trucks, H. B. Schlegel, P. M. W. Gill, B. G. Johnson, M. A. Robb, J. R. Cheeseman, T. A. Keith, G. A. Petersson, J. A. Montgomery, K. Raghavachari, M. A. Al-Laham, V. G. Zakrzewski, J. V. Ortiz, J. B. Foresman, J. Cioslowski, B. B. Stefanov, A. Nanayakkara, M. Challacombe, C. Y. Peng, P. Y. Ayala, W. Chen, M. W. Wong, J. L. Andres, E. S. Replogle, R. Gomperts, R. L. Martin, D. J. Fox, J. S. Binkley, D. J. Defrees, J. Baker, J. J. P. Stewart, M. Head-Gordon, C. Gonzales, and J. A. Pople, Gaussian, Inc., Pittsburgh PA, 1995.
[67] R. Krishnan, J. S. Binkley, R. Seeger, and J. A. Pople, J. Chem. Phys. **72**, 650 (1980).
[68] A. D. McLean and G. S. Chandler, J. Chem. Phys. **72**, 5639 (1980).
[69] T. Clark, J. Chandrasekhar, G. W. Spitznagel, and P. v. R. Schleyer, J. Comput. Chem. **4**, 294 (1983).
[70] M. J. Frisch, J. A. Pople, and J. S. Binkley, J. Chem. Phys. **80**, 3265 (1984).
[71] W. R. Wadt and P. J. Hay, J. Chem. Phys. **82**, 284 (1985).
[72] P. J. Hay and W. R. Wadt, J. Chem. Phys. **82**, 299 (1985).
[73] L. S. Cederbaum, J. Phys. B **8**, 290 (1975).
[74] W. von Niessen, J. Shirmer, and L. S. Cederbaum, Comput. Phys. Rep. **1**, 57 (1984).
[75] V. G. Zakrzewski and W. von Niessen, J. Comput. Chem. **14**, 13 (1993).
[76] V. G. Zakrzewski and J. V. Ortiz, Int. J. Quantum Chem. **53**, 583 (1995).
[77] J. V. Ortiz, V. G. Zakrzewski, and O. Dolgunitcheva, in *Conceptual Trends in Quantum Chemistry*, edited by E. S. Kryachko (Kluwer, Dordrecht, 1997), Vol. 3, p. 463.
[78] The better agreement between our results at the OVGF level of theory and the experimental data than the results of Scheller and Cederbaum was due to cancellations of two errors in our calculations. One came from the limitation of our one-electron basis sets and another one (opposite sign) was due to the less complete account of the electron correlation effects in the OVGF method. Such cancellation did not happen in the Scheller and Cederbaum calculations. However, differences between the two calculations (0.2 eV) are really quite small.
[79] J. V. Ortiz, in *Computational Chemistry: Reviews of Current Trends*, edited by J. Leszczynski (World Scientfic, Singapore, 1997), Vol. 2, pp. 1–61.
[80] G. L. Gutsev and A. I. Boldyrev, J. Phys. Chem. **94**, 2256 (1990).
[81] G. L. Gutsev and A. I. Boldyrev, Russ. J. Phys. Chem. **63**, 2116 (1989).
[82] K. P. Huber and G. Herzberg, *Molecular Spectra and Molecular Structure IV: Constants of Diatomic Molecules* (Van Nostrand Reinhold, New York, 1979).
[83] J. Berkowitz, C. H. Batson, and G. L. Goodman, J. Chem. Phys. **71**, 2624 (1979).
[84] T. M. Miller, D. G. Leopold, K. K. Murray, and W. C. Lineberger, J. Chem. Phys. **85**, 2368 (1986).
[85] A. W. Potts, T. A. Williams, and W. C. Prince, Proc. R. Soc. London, Ser. A **341**, 147 (1974).

Downloaded 23 May 2003 to 155.101.19.15. Redistribution subject to AIP license or copyright, see http://ojps.aip.org/jcpo/jcpcr.jsp